

Solution of a Multiple-Scattering Inverse Problem: Electron Diffraction from Surfaces

D. K. Saldin,¹ A. Seubert,² and K. Heinz²

¹*Department of Physics, University of Wisconsin–Milwaukee, P.O. Box 413, Milwaukee, Wisconsin, 53201*

²*Lehrstuhl für Festkörperphysik, Universität Erlangen–Nürnberg, Staudtstrasse 7, D-91058 Erlangen, Germany*

(Received 14 November 2001; published 5 March 2002)

We present a solution to the multiple-scattering inverse problem for low-energy electron diffraction that enables the determination of the three-dimensional atomic structure of an entire surface unit cell directly from measured data. The solution requires a knowledge of the structure of the underlying bulk crystal and is implemented by a maximum entropy algorithm.

DOI: 10.1103/PhysRevLett.88.115507

PACS numbers: 61.14.Dc, 61.14.Hg, 68.43.Fg

In many branches of science, ranging from astronomy to crystallography, the characteristics of a physical object are inferred from the angular variation of the intensity of radiation received from it. Provided the object may be regarded as real (in the mathematical sense) and the measured quantities the square moduli of their (invertible) Fourier transforms, the former may be deduced from the data by exploiting probability estimates of the combined phases associated with the dominant intensities [1], by an oversampling of the data at a density greater than the Nyquist criterion [2], or by an exploitation of a knowledge of part of the structure [3].

When multiple scattering is dominant, as in the case of electron diffraction from a crystal, the absence of a simple invertible relationship between an object and a scattered amplitude presents a much greater challenge for the development of an inverse method. There have been several recent proposals for such methods for the solution of *projected* crystal structures in high-energy electron diffraction [4]. To some extent, the direct solution of three-dimensional (3D) structures from multiply scattered radiation has been addressed in atomic-source electron holography [5] by algorithms designed to lock into the single-scattering component of a multiple-scattering interference pattern, essentially by a method of matched filtering [6]. However, due to the decay of object wave amplitudes with the inverse of the distance from the source, augmented by a short inelastic scattering length, such methods tend to reveal the structure of only a rather local region around the source [7]. In the present Letter, we demonstrate the solution of the multiple-scattering inverse problem for the determination of the 3D atomic structure of an entire surface unit cell in the more classic crystallographic geometry of a distant external source of radiation incident on a single sample orientation, as exemplified by the case of low-energy electron diffraction (LEED) [8] from a crystal surface.

The solution exploits several key ideas: the *first* is the ability to divide the scattering paths into a subset that scatters from only a known part of the structure, and another that includes scattering from the unknown part. For LEED we can draw on a holographic analogy in which the

dynamical (or multiple-scattering) structure factor F_ϵ (or scattering amplitude from a repeating unit of the surface due to an incident plane wave of unit amplitude) may be regarded as a sum

$$F_\epsilon = R_\epsilon + S_\epsilon \quad (1)$$

of a known reference wave R_ϵ solely from scattering by the deeper, or bulk, layers, whose structure is assumed known, and an object wave S_ϵ involving scattering from the unknown surface layers (where ϵ is an index specifying a data point). The *second* key is the ability to represent the total object wave as a linear combination

$$S_\epsilon = \sum_j p_j O_{\epsilon j} \quad (2)$$

of *calculable elementary object waves* $O_{\epsilon j}$ [9]. In the case of LEED, each of these consists of a *renormalized structure factor* of a test layer consisting of a 2D primitive superlattice, containing an atom at a given position j relative to the bulk crystal. The *third* key is the interpretation of the set of non-negative coefficients $\{p_j\}$ of this expansion as a spatial distribution of the unknown scattering elements, which may be computed from the measured diffraction data by a maximum entropy algorithm. In LEED these scattering elements are primitive sublattices of 2D periodicity, and $\{p_j\}$ may be regarded as the spatial distribution of atoms within a surface unit cell. We develop these ideas in what follows.

Consider the scattering of an electron from a surface consisting of an ordered atomic layer above a crystal substrate. We assume that the structure of the substrate is known and thus that it is possible to calculate exactly the scattering matrix \mathbf{B}^{-+} in a plane-wave basis of the surface repeat unit from a standard LEED program [10]. In the usual LEED notation, we describe the corresponding scattering matrices of the test layer by $\mathbf{M}^{\pm\pm}$, where the second (first) superscript denotes the direction of the flux of the incident (scattered) wave with + (−) defined towards the bulk (vacuum). Exploiting the weakness of backscattering processes compared to forward ones, the scattering paths involving the test layer and the substrate may be ordered by the number of backscattering events. The minimum

number of backscattering processes in a propagation path of a detectable LEED electron is one. Also, exploiting the weakness of $\sim 90^\circ$ scattering of electrons of normal incidence (usually employed in LEED) compared with either forward or backscattering, we approximate the scattering matrices $\mathbf{M}^{\pm\pm}$ by “kinematic” or (single-scattering) expressions that neglect multiple scattering within the test layer [11]. Define an origin O at the vacuum edge of the surface, a height h above the uppermost atomic layer of the substrate (see Fig. 1). The propagation of electrons below this layer must take account of both refraction and absorption. Let B be the origin assumed for the definition of the bulk reflection matrix \mathbf{B}^{-+} . If a matrix (also in the plane-wave representation) for the propagation of an electron from a general point C to another one D is defined as \mathbf{P}_{DC} , we may write

$$R_\epsilon = (\mathbf{P}_{OB}\mathbf{B}^{-+}\mathbf{P}_{BO})_{\mathbf{g}\mathbf{0}}, \quad (3)$$

where the outer indices $\mathbf{g}\mathbf{0}$ specify the matrix elements for scattering from the incident beam into the Bragg spot index \mathbf{g} , and ϵ represents the combination of \mathbf{g} and the electron energy E . Also, to first order in scattering from the test layer,

$$O_{\epsilon j} \approx O_{\epsilon j}^{(1)} + O_{\epsilon j}^{(2)} + O_{\epsilon j}^{(3)}, \quad (4)$$

where

$$O_{\epsilon j}^{(1)} = (\mathbf{P}_{Oj}\mathbf{M}^{-+}\mathbf{P}_{jO})_{\mathbf{g}\mathbf{0}} \quad (5)$$

is the bare scattering matrix element, and

$$O_{\epsilon j}^{(2)} = (\mathbf{P}_{OB}\mathbf{B}^{-+}\mathbf{P}_{Bj}\mathbf{M}^{++}\mathbf{P}_{jO})_{\mathbf{g}\mathbf{0}} \quad (6)$$

and

$$O_{\epsilon j}^{(3)} = (\mathbf{P}_{Oj}\mathbf{M}^{--}\mathbf{P}_{jB}\mathbf{B}^{-+}\mathbf{P}_{BO})_{\mathbf{g}\mathbf{0}} \quad (7)$$

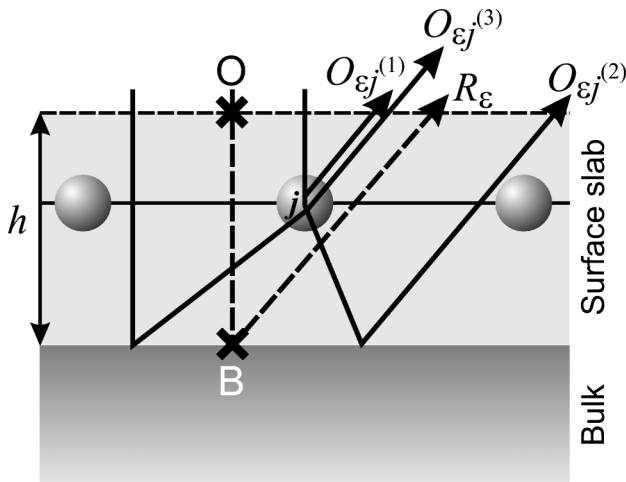


FIG. 1. Electron propagation and scattering paths giving rise to the reference wave R_ϵ and three dominant contributions $O_{\epsilon j}^{(1)}$, $O_{\epsilon j}^{(2)}$, $O_{\epsilon j}^{(3)}$ to an elementary object wave $O_{\epsilon j}$ due to scattering from a primitive test 2D lattice with an atom at j in a surface slab of height h above the outermost bulk layer.

are the extra contributions to the renormalized matrix element (or structure factor) that include the dominant multiple scattering between the test layer and the bulk. Representative scattering paths followed by electrons contributing to R_ϵ , $O_{\epsilon j}^{(1)}$, $O_{\epsilon j}^{(2)}$, and $O_{\epsilon j}^{(3)}$ are illustrated in Fig. 1. Since the theory involves a single test lattice, multiple scattering between different sublattices constituting the real surface slab is neglected. Comparisons with full multiple-scattering calculations have shown this to be a reasonable approximation, even for the severe test below of normal incidence on CO molecules oriented normal to a surface. All matrices on the right-hand side (RHS) of (3)–(7) need to be evaluated at an energy of $E - V_{0r}$, where V_{0r} is the (negative) real part of the potential step at the surface [8].

If a LEED structure factor may be written in the form given by (1)–(7), determination of the distribution $\{p_j\}$ from constraints imposed by the experimental data would give the positions of atoms within a slab representing the surface unit cell [9]. The maximum entropy method [12–14] provides a prescription for recovering this distribution from incomplete and noisy data. It is based on the maximization of the functional

$$Q[\{p_l^{(n)}\}] = - \sum_l p_l^{(n)} \ln \left[\frac{p_l^{(n)}}{e p_l^{(n-1)}} \right] - \frac{\lambda'}{2} \chi^2 \quad (8)$$

of the estimate $\{p_l^{(n)}\}$ of the distribution at iteration n . The first term on the RHS of (8) represents the entropy of $\{p_l^{(n)}\}$ relative to its estimate $\{p_l^{(n-1)}\}$ at the previous iteration [15] (where e is base of natural logarithms), while the second term contains the Lagrange multiplier λ' and the *chi-squared statistic*

$$\chi^2 = \frac{1}{N} \sum_\epsilon \frac{|S_\epsilon^{(n)} - T_\epsilon^{(n-1)}|^2}{\sigma_\epsilon^2}, \quad (9)$$

with N the number of data points and σ_ϵ the estimated uncertainty in the measured structure factor amplitude $|F_\epsilon|$. The quantity χ^2 constrains the theoretical estimate of the total object wave

$$S_\epsilon^{(n)} = \sum_l p_l^{(n)} O_{\epsilon l} \quad (10)$$

to the experimental one

$$T_\epsilon^{(n-1)} = |F_\epsilon| \exp[i\phi_\epsilon^{(n-1)}] - R_\epsilon, \quad (11)$$

where the current estimate of the unmeasured phase $\phi_\epsilon^{(n-1)}$ associated with the experimental amplitude $|F_\epsilon|$ is determined by the distribution $\{p_j^{(n-1)}\}$ via (10) and

$$\phi_\epsilon^{(n-1)} = \arg[R_\epsilon + S_\epsilon^{(n-1)}]. \quad (12)$$

Q may be maximized by requiring that

$$\frac{\partial Q}{\partial p_j^{(n)}} = 0 \quad \forall j. \quad (13)$$

After some algebra one obtains the set of equations

$$p_j^{(n)} = p_j^{(n-1)} \exp[-\lambda\{\mu_j^{(n-1)} - \tau_j^{(n-1)}\}], \quad (14)$$

where

$$\mu_j^{(n-1)} = \frac{1}{N} \sum_{\epsilon} \text{Re}\{S_{\epsilon}^{(n-1)} O_{\epsilon j}^*\} \quad (15)$$

and

$$\tau_j^{(n-1)} = \frac{1}{N} \sum_{\epsilon} \text{Re}\{T_{\epsilon}^{(n-1)} O_{\epsilon j}^*\} \quad (16)$$

provided that all the variances σ_{ϵ}^2 can be replaced by their mean value $\langle\sigma_{\epsilon}^2\rangle$ and $\lambda = \lambda'/\langle\sigma_{\epsilon}^2\rangle$ is sufficiently small [14,16]. The algorithm is initiated at iteration $n = 1$ by taking $\{p_j^{(0)}\}$ to be the least biased *uniform* distribution normalized to the expected number N_a of atoms in the surface unit cell and by using this expression to evaluate $\mu_j^{(0)}$ and $\tau_j^{(0)}$ via (10)–(12) and (15)–(16). After completion of each iteration, the new distribution is renormalized to the same expected number of atoms. Equation (14) shows that if all elements of $\{p_j^{(0)}\}$ are non-negative, so will be all elements $\{p_j^{(n)}\}$ at any subsequent iteration.

We tested the algorithm first on “pseudoeperimental” data obtained by simulating, by means of a standard computer program [10], LEED I/E data for the accepted model of the $c(2 \times 2)\text{CO}/\text{Ni}(001)$ [17,18]. Also required as input to the calculation of the reference wave R_{ϵ} is the reflection matrix \mathbf{B}^{-+} of the bulk-terminated substrate, computed by the same program. The calculations of the propagation matrices, e.g., \mathbf{P}_{jO} , for the evaluation of R_{ϵ} and $O_{\epsilon j}$ from (3) and (4), respectively, require only the evaluation of complex exponentials with arguments containing the (complex) wave vectors of the plane-wave expansions between the atomic layers and the vectors relating the fixed reference positions O and B , and the positions, j , of origin atoms of the test surface layer. The elementary object waves $O_{\epsilon j}$ are computed from (4)–(7), taking $\mathbf{M}^{\pm\pm}$ to be the kinematic scattering matrices of a $c(2 \times 2)$ superlattice of oxygen atoms. The algorithm (14) was first executed to convergence after 30 iterations with the summations (15) and (16) for $\mu_j^{(n-1)}$ and $\tau_j^{(n-1)}$ over data only in the so-called *integer-order* Bragg spots which have a nonzero contribution from the reference amplitudes R_{ϵ} . This gave rise to the so-called *average structure* where the true superstructure is replaced by its average in each of its constituent unit cells of the bulk 2D periodicity [14]. Starting phases $\phi_{\epsilon}^{(30)}$ of the *fractional-order* (or superstructure) spots were obtained by interpolation of the arguments of $S_{\epsilon}^{(30)}$ from the neighboring integer-order spots, and the algorithm resumed with the inclusion also of “experimental” fractional-order data until a new convergence after a further 70 iterations. The distribution of $\{p_j^{(n)}\}$ over a 3D surface slab of height 3.20 Å and lateral extent equal to a little more than a (2×2) unit cell after a total of 100 iterations is depicted in Fig. 2. Despite the fact that $O_{\epsilon j}$ was

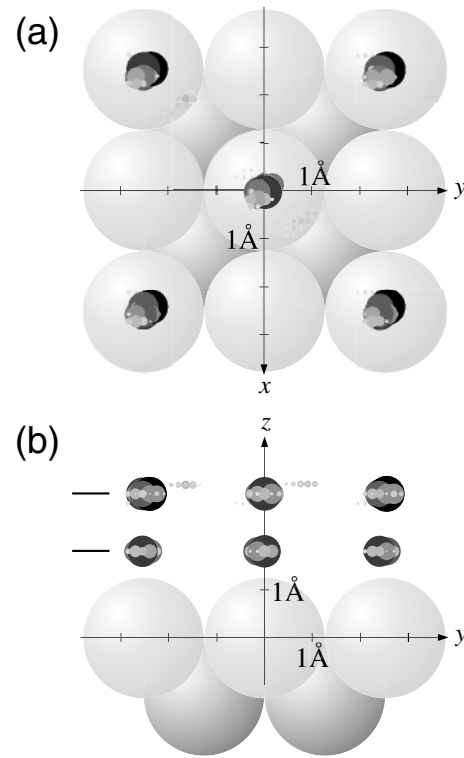


FIG. 2. Plan view (a) and side elevation (b) of the 3D distribution $\{p_j\}$ above a Ni(001) surface after convergence of the maximum entropy algorithm applied to pseudoeperimental LEED data from $c(2 \times 2)\text{-CO}/\text{Ni}(001)$. The radii and the darkness of the small spheres at each point j on a uniform grid of $39 \times 39 \times 12$ points covering a surface slab above the substrate are proportional to the calculated value of p_j . The figures reveal the correct structure of CO molecules aligned perpendicular to the substrate and adsorbed in on-top sites. The short horizontal lines at the left in (b) indicate the heights of the C and O atoms above the surface assumed in the model.

calculated from a test layer consisting of a primitive 2D lattice of a single atomic species (due to the similarity of C and O scattering factors, which of these species is taken to represent the test layer is almost immaterial) the algorithm is able to recover the positions of both the C and O atoms of the molecules oriented normal to the surface and adsorbed on the “on-top” sites directly above Ni atoms of the outermost substrate layer, as assumed in the model.

For a test with experimental LEED data, we chose the surface of $c(2 \times 2)\text{Br}/\text{Pt}(110)$. A recent study of possible Br adsorption sites by conventional LEED [19], which considered on-top, hollow, as well as long- and short-bridge locations, found good agreement between experiment and theory only for adsorption on the short-bridge sites of a *slightly* relaxed, buckled, and reconstructed substrate. Computer time limitations prevented an exhaustive examination of all possible structures. In contrast, in a real sense, our method represents a *model-independent* determination of the adsorption geometry from the same data [19]. With the reference wave R_{ϵ} calculated from (3) with \mathbf{B}^{-+} from an ideal bulk-terminated model of the Pt(110) substrate,

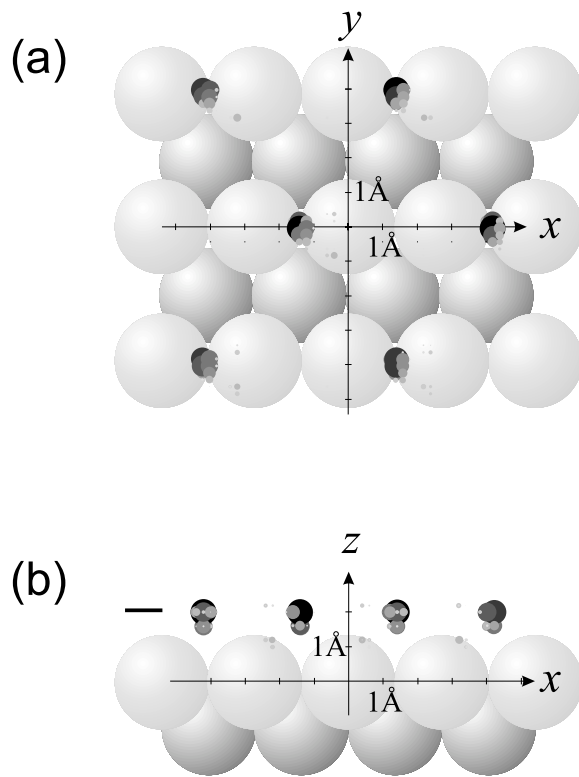


FIG. 3. Same as Fig. 2 except that $\{p_j\}$ here represents the calculated 3D distribution on a grid of $45 \times 45 \times 8$ points above a Pt(110) surface after convergence of the maximum entropy algorithm operating on experimental LEED data from $c(2 \times 2)$ -Br/Pt(110) [19]. The figures reveal both the correct short-bridge adsorption sites of the Br atoms, and their height above the substrate as determined by a conventional analysis [19], indicated by the short horizontal line in (b).

and a surface slab height of 2.40 \AA , the algorithm was run initially until convergence after 350 iterations with just the data in the integer-order Bragg spots. After interpolation at each energy of the resulting phases of S_ϵ to give initial estimates of the phases of the fractional-order amplitudes, the algorithm was resumed until final convergence after a further 225 iterations. The result is an unambiguous independent confirmation of the short-bridge adsorption site, and even an excellent reproduction of the height of the $c(2 \times 2)$ Br adsorbate layer, as determined by the conventional LEED analysis (see Fig. 3). For substrates with significant surface relaxations or reconstructions, if R_ϵ is computed from the scattering of just the deeper unreconstructed bulk, the distribution of $\{p_j^{(n)}\}$ in the surface slab may reveal even the structure of the outermost layers, as in x-ray diffraction [14].

The calculations of the results of Figs. 2 and 3 required less than an hour on a modern computer workstation. The scattering matrices $\mathbf{M}^{\pm\pm}$ were computed at run time from input phase shifts of the atoms constituting the test layer. The bulk reflection matrices \mathbf{B}^{-+} were calculated rapidly from a single run of a standard LEED computer program. Essentially no assumption was made about the adsorbate

structure, save the lateral dimensions of the surface unit cell suggested by the form of the diffraction pattern. Only as many reference matrices R_ϵ needed to be calculated as there are distinct energies at which data are measured, and only as many elementary object matrices $O_{\epsilon j}$ as this number multiplied by the number of grid points j within a symmetry-reduced sector of the surface unit cell. This product is *independent of the structural complexity of the unit cell*. As demonstrated in the example above of CO/Ni(001), the algorithm is able to recover the positions of multiple atoms per surface unit cell even with a single test layer: in such a case, the distribution $\{p_j\}$ is simply multiply peaked in the unit cell. The roadblock posed by the practically insuperable problem of nonpolynomial scaling of trial-and-error model fitting methods [20] may thus be bypassed.

This work was supported by NSF Grants No. DMR-9815092 and No. DMR-9972958-001, DOE Grants No. DE-FG02-84ER45076 and No. DE-FG02-01ER45926, and the Deutsche Forschungsgemeinschaft (DFG) through Sonderforschungsbereich 292.

-
- [1] C. Giacovazzo, *Direct Methods in Crystallography* (Academic, London, 1980).
 - [2] J. R. Fienup, *Appl. Opt.* **21**, 2758 (1982).
 - [3] A. Szöke, *Acta Crystallogr. Sect. A* **49**, 853 (1993).
 - [4] J. C. H. Spence, *Acta Crystallogr. Sect. A* **54**, 7 (1998); L. J. Allen, T. W. Josefsson, and H. Leeb, *ibid.* **54**, 388 (1998); W. Sinkler, E. Bengu, and L. D. Marks, *ibid.* **54**, 591 (1998).
 - [5] See, e.g., J. J. Barton, *Phys. Rev. Lett.* **67**, 3106 (1991); K. Heinz, A. Seubert, and D. K. Saldin, *J. Phys. Condens. Matter* **13**, 10647 (2001).
 - [6] L. A. Wainstein and V. D. Zubakov, *Extraction of Signals from Data* (Dover, New York, 1970).
 - [7] K. Reuter *et al.*, *Phys. Rev. Lett.* **79**, 4818 (1997).
 - [8] J. B. Pendry, *Low Energy Electron Diffraction* (Academic, London, 1974).
 - [9] A. Szöke, *Phys. Rev. B* **47**, 14044 (1993).
 - [10] M. A. Van Hove and S. Y. Tong, *Surface Crystallography by LEED* (Springer, Berlin, 1979).
 - [11] This *quasidynamical* approximation has been successfully employed also in conventional LEED analyses; see, e.g., N. Bickel and K. Heinz, *Surf. Sci.* **163**, 435 (1985).
 - [12] E. T. Jaynes, *Phys. Rev.* **106**, 620 (1957).
 - [13] D. M. Collins, *Nature (London)* **298**, 49 (1982).
 - [14] D. K. Saldin *et al.*, *Comput. Phys. Commun.* **137**, 12 (2001).
 - [15] L. D. Landau and E. M. Lifshitz, *Statistical Physics* (Pergamon, New York, 1980).
 - [16] V. L. Shneerson, D. L. Wild, and D. K. Saldin, *Acta Crystallogr. Sect. A* **57**, 163 (2001).
 - [17] K. Heinz, E. Lang, and K. Müller, *Surf. Sci.* **87**, 595 (1979).
 - [18] L. G. Petersson *et al.*, *Phys. Rev. Lett.* **42**, 1545 (1979).
 - [19] V. Blum *et al.*, *Phys. Rev. B* (to be published).
 - [20] J. B. Pendry, K. Heinz, and W. Oed, *Phys. Rev. Lett.* **61**, 2953 (1988).